



HHS Public Access

Author manuscript

Annu Int Conf IEEE Eng Med Biol Soc. Author manuscript; available in PMC 2021 October 26.

Published in final edited form as:

Annu Int Conf IEEE Eng Med Biol Soc. 2020 July ; 2020: 1803–1806. doi:10.1109/EMBC44109.2020.9175691.

Adaptable Sensor Arrays for Fetal Magnetocardiographic Measurements Using Optically-Pumped Magnetometers: A Pilot Study

Diana Escalona-Vargas [Member, IEEE],

Department of Pediatrics, University of Arkansas for Medical Sciences

Hari Eswaran [Member, IEEE]

Department of Obstetrics and Gynecology, University of Arkansas for Medical Sciences, Little Rock, AR 72205 USA

Abstract

Fetal magnetocardiography (fMCG) is a non-invasive method of measuring magnetic signals generated by the depolarizing heart. fMCG has proved to have superior signal-to-noise ratio characteristics and enables precise detection of the R-R intervals for fetal heart rate variability (FHRV) analysis. FHRV is one of the most useful clinical indicators for investigating fetal neurodevelopment. Currently, fMCG recordings rely on superconducting quantum interference devices (SQUIDs) which require cryogenics leading to a high cost device. New cryogenic-free sensors called optical pump magnetometers (OPMs) have emerged as alternative to SQUIDs. To take advantage of the flexibility of the OPM sensors, we explored the ability of OPM sensors to measure the fMCG at different maternal positions and sensor locations. Data were collected with a 14-channel OPM array using different sitting positions (mother leaning forward, backward, and prone). Projection operator algorithm based on minimum norm (POMN) was applied to extracted fMCG. R peaks were obtained to perform standard FHRV analysis. We were able to configure a standalone array of the OPMs that conforms to the shape of the maternal abdomen to obtain signals with sufficient quality. We extracted and quantified FHRV parameters in three low-risk fetuses. Results showed that FHRV values are in the range of previous SQUID studies.

I. INTRODUCTION

Fetal magnetocardiography (fMCG) is a non-invasive method of measuring magnetic signals generated by the depolarizing heart. The tracings derived from fMCG appear similar to fetal electrocardiograms (ECG) [1], and studies have shown that electrical and magnetic signals have similar morphological characteristics for the P-wave, QRS complex, and T-wave [2]. fMCG is acquired using Superconducting Quantum Interference Devices (SQUIDs) [3] allowing high signal-to-noise ratio (SNR) compared with fetal ECG where signals are effected due to the vernix caseosa and insulating maternal tissues [4]. fMCG has proved to have superior SNR characteristics even though there has been improvement of fetal ECG equipment and sensors. Although abdominal fetal ECG is commercially available and is

a relatively inexpensive tool for fetal monitoring, technical challenges still remain. The American Heart Association recently acknowledged the academic and clinical usefulness of fMCG [5].

It has been shown that fMCG is capable of accurately and reliably detecting cardiac rhythm [6], [7]. The temporal resolution of the QRS complex detection of fMCG enables precise fetal heart rate variability (FHRV) analysis from R-R intervals, and reflects the normal/pathologic state of the fetuses. Changes in FHRV values are thought to be associated with the development of the autonomic nervous system [8].

Currently, fMCG recordings rely on ultrasensitive SQUIDs which require cryogenics and a bulky magnetically shielded room, leading to a high cost device; they are also fixed in space. In this context, new cryogenic-free sensors called optical pump magnetometers (OPMs) have emerged as alternative to SQUID sensors. Previous studies have measured fetal biomagnetic signals using OPM sensors [9], [10]. A study reported by our group [11], demonstrated a direct comparison of signal morphology in simultaneously recordings of fMCG with the SQUID technology. To take advantage of the flexibility of the OPM sensors, in this work we explored the ability of OPM sensors to record the fMCG at different maternal positions and sensor locations. We provided details about the OPM fMCG measurements and signal processing. We presented FHRV extracted from the OPM signals.

II. METHODS

A. Measurements

Data was recorded for 6 minutes from 3 healthy pregnant women with a 14-channel OPM array. Sensors were positioned in the radial direction to lightly touch maternal abdomen. Previous to OPM recording, an ultrasound was performed to localize the fetal heart. This study was approved by the Institutional Review Board, and all the participants provided written informed consent to participate.

To take advantage of the conformal and geometric flexibility of the OPM sensors, the OPM signals were measured with three different maternal positions and sensor locations:

1. **Leaning backward:** The subject sat comfortably on a reclining chair where OPM sensors were positioned in a curved belt and leaning backwards on a chair (Fig. 1A).
2. **Leaning forward:** The subject sat comfortably on a seat leaning forward on a curved grid (see Fig 1B). OPM sensors were positioned on the layout in the middle row which contains most the fetal heart signals according to the ultrasound.
3. **Prone position:** The subject lies flat in a customized wooden bed with a pregnancy pillow. The OPM array is in contact with the abdomen from below with a curved grid (Fig. 1C).

The grid (see Fig. 1D, left) corresponds to a 3D-printing holder that contains 5 rows to accommodate up to 26 sensors (3 upper rows with 6 sensors holders each, and 2 lower rows

with 4 sensors holders each). Belts (see Fig. 1D, right) are two 3D-printing flexible holders to allocate 10 sensors each. The spacing between sensor holders was 3 cm. The belts were held over the maternal abdomen with flexible elastic straps.

B. Signal processing

OPM signals were band-pass filtered between 0.5-50 Hz and notch filtered for power line attenuation. To obtain the fMCG signal from OPM data, projection operator algorithm based on minimum norm (POMN) was applied to attenuate the maternal cardiac signals (mMCG) [12]. Next, we detrended the fMCG data using a wavelet transform approach [13].

OPMN method has the advantage of either removing the mMCG or obtained pure fMCG signals, and causes less signal redistribution within sensor space compared with regular projection operator (OP) algorithm [14]. In this work, we used the covariance version of OPMN as follows:

1. Removed the maternal MCG traces ($mMCG_2$) using OP method [14] from raw data (B_{raw}) to build a preliminary model for the fetal heart activity data ($fMCG_2$)
2. R peaks (R_f) from $fMCG_2$ are obtained via a peakdetection algorithm [15]
3. Time-averaged signals (M_{OPMN}) are calculated using the R_f peaks from $fMCG_2$
4. A projector operator is calculated as follows:

$$P_{OPMN} = (M_{OPMN} M_{OPMN}^T) (A_c + sf Tr(A_c) I)^{-1}$$
, where $sf = 10^{-5}$, A_c is the covariance matrix of B_{raw} , and $Tr(\cdot)$ denotes the matrix trace operator.
5. To obtain only pure fMCG data ($fMCG_1$), the covariance projection operator is applied to B_{raw} as follows: $fMCG_1 = P_{OPMN} B_{raw}$

C. fMCG indicators

The R peaks of the fMCG traces were obtained via a peak-detection algorithm [15]. Standard fetal heart rate variability metrics were quantified: FHR (beats per minute, bpm), R-R intervals (millisecond, ms), root mean square of successive differences (RMSSD, ms) and standard deviation of normal-to-normal beat intervals (SDNN, ms). FHR and R-R intervals are influenced by both parasympathetic (vagal) and sympathetic activity. RMSSD quantify the short term variability, and SDNN measures overall variability of sympathetic and vagal oscillations. FHRV indicators were extracted from the first 300 seconds of fMCG data.

III. RESULTS AND DISCUSSION

We successfully recorded biomagnetic signals from 3 participants at one of the three sitting positions between 34 to 36 weeks of gestational age (GA). Participants were 21 ± 2 years with BMI 30 ± 1 kg/m^2 , all were Black/African American, and 67% of babies were males.

Fig. 2 shows a representative block of 7-sec time series of the measurements in the three positions at 34 (forward), 35 (backward) and 36 (prone) weeks GA. Fig. 2 shows the raw data (Fig. 2A, 2C and 2E) and the corresponding extracted fMCG signals (Figs. 2B, 2D and 2F).

2F) with amplitudes around 2 and 4 pT (pico-Tesla). Dots on the top of Figs. 2A, 2C and 2E represent the positions of the maternal (green) and fetal (blue) R peaks. In Fig. 2A the artifact contributions due to maternal breathing (around 5Hz) can be observed.

For each dataset, R-R intervals are shown in Fig. 3A-3C, and FHRV values are shown in Table 1. Grand average and standard deviation values of R-R intervals and FHR were: 444.14 ± 12.8 ms and 135.4 ± 3.9 bpm, respectively. RMSSD and SDNN were 5.1 ± 1.9 ms and 17.2 ± 6.4 ms, respectively. All FHRV parameters are in range of previous SQUID fMCG studies [16], [17], [18], [19].

IV. CONCLUSIONS AND FUTURE DIRECTIONS

We were able to configure a stand-alone array of the OPMs that conforms to the shape of the maternal abdomen to obtain signals with sufficient quality for fetal applications. We extracted and quantified FHR variability parameters in three low-risk fetuses. Results showed that fetal heart rate variability values in the range of previous studies. We plan to expand the number of subjects where data will be collected serially with different maternal and sensor positions. Future development in OPM systems are geared towards sensor size reduction and smaller shielding room systems [20] that could be potentially increase the use of biomagnetic sensors for fetal-maternal studies.

Acknowledgments

This work was supported by the U.S. National Institute of Health (NIH) under Grant R21HD091744.

REFERENCES

- [1]. Kariniemi V, Ahopelto J, Karp PJ, and Katila T, "The fetal magnetocardiogram," 1974.
- [2]. saarinen M, siltanen P, Karp P, and Katila T, "The normal magnetocardiogram: I morphology." *Annals of clinical research*, vol. 10, pp. 1–43, 1978.
- [3]. Vrba J, "Multichannel SQUID biomagnetic systems," in *Applications of superconductivity*. Springer, 2000, pp. 61–138.
- [4]. Dawes G, Moulden M, and Redman C, "Limitations of antenatal fetal heart rate monitors," *American journal of obstetrics and gynecology*, vol. 162, no. 1, pp. 170–173, 1990. [PubMed: 2301488]
- [5]. Donofrio MT, Moon-Grady AJ, Hornberger LK, Copel JA, Sklansky MS, Abuhamad A, Cuneo BF, Huhta JC, Jonas RA, Krishnan A et al. "Diagnosis and treatment of fetal cardiac disease," *Circulation*, vol. 129, no. 21, pp. 2183–2242, 2014. [PubMed: 24763516]
- [6]. Leuthold A, Wakai RT, and Martin CB, "Noninvasive in utero assessment of PR and QRS intervals from the fetal magnetocardiogram," *Early human development*, vol. 54, no. 3, pp. 235–243, 1999. [PubMed: 10321790]
- [7]. Lowery CL, Campbell JQ, Wilson JD, Murphy P, Preissl H, Malak SF, and Eswaran H, "Noninvasive antepartum recording of fetal st segment with a newly developed 151-channel magnetic sensor system," *American journal of obstetrics and gynecology*, vol. 188, no. 6, pp. 1491–1497, 2003. [PubMed: 12824983]
- [8]. Berntson GG, Thomas Bigger J, Eckberg DL, Grossman P, Kaufmann PG, Malik M, Nagaraja HN, Porges SW, Saul JP, Stone PH et al. "Heart rate variability: origins, methods, and interpretive caveats," *Psychophysiology*, vol. 34, no. 6, pp. 623–648, 1997. [PubMed: 9401419]
- [9]. Wyllie R, Kauer M, Wakai RT, and Walker TG, "Optical magnetometer array for fetal magnetocardiography," *Optics letters*, vol. 37, no. 12, pp. 2247–2249, 2012. [PubMed: 22739870]

- [10]. Alem O, Sander TH, Mhaskar R, LeBlanc J, Eswaran H, Steinhoff U, Okada Y, Kitching J, Trahms L, and Knappe S, "Fetal magnetocardiography measurements with an array of microfabricated optically pumped magnetometers," *Physics in Medicine & Biology*, vol. 60, no. 12, p. 4797, 2015. [PubMed: 26041047]
- [11]. Eswaran H, Escalona-Vargas D, Bolin EH, Wilson JD, and Lowery CL, "Fetal magnetocardiography using optically pumped magnetometers: a more adaptable and less expensive alternative?" *Prenatal diagnosis*, vol. 37, no. 2, pp. 193–196, 2017. [PubMed: 27891637]
- [12]. Wilson JD and Haueisen J, "Separation of physiological signals using minimum norm projection operators," *IEEE Transactions on Biomedical Engineering*, vol. 64, no. 4, pp. 904–916, 2016. [PubMed: 27337708]
- [13]. Addison PS, "Wavelet transforms and the ecg: a review," *Physiological measurement*, vol. 26, no. 5, p. R155, 2005. [PubMed: 16088052]
- [14]. Vrba J, Robinson SE, McCubbin J, Lowery CL, Eswaran H, Wilson JD, Murphy P, and Preißl H, "Fetal MEG redistribution by projection operators," *Biomedical Engineering, IEEE Transactions on*, vol. 51, no. 7, pp. 1207–1218, 2004.
- [15]. Ulsar U, Govindan RB, Wilson J, Lowery C, Preissl H, and Eswaran H, "Adaptive rule based fetal qrs complex detection using hilbert transform," in *Conference proceedings: Annual International Conference of the IEEE Engineering in Medicine and Biology Society. IEEE Engineering in Medicine and Biology Society*, vol. 2009, 2009, p. 4666.
- [16]. Van Leeuwen P, Lange S, Bettermann H, Grönemeyer D, and Hatzmann W, "Fetal heart rate variability and complexity in the course of pregnancy," *Early human development*, vol. 54, no. 3, pp. 259–269, 1999. [PubMed: 10321792]
- [17]. Govindan R, Lowery CL, Campbell JQ, Best TH, Murphy P, Preissl HT, and Eswaran H, "Early maturation of sinus rhythm dynamics in high-risk fetuses," *American journal of obstetrics and gynecology*, vol. 196, no. 6, pp. 572–e1, 2007. [PubMed: 17547900]
- [18]. Van Leeuwen P, Cysarz D, Edelhäuser F, and Grönemeyer D, "Heart rate variability in the individual fetus," *Autonomic Neuroscience*, vol. 178, no. 1-2, pp. 24–28, 2013. [PubMed: 23369622]
- [19]. Escalona-Vargas D, Wu H.-t., Frasch MG, and Eswaran H, "A comparison of five algorithms for fetal magnetocardiography signal extraction," *Cardiovascular engineering and technology*, vol. 9, no. 3, pp. 483–487, 2018. [PubMed: 29582244]
- [20]. Iivanainen J, Zetter R, Grön M, Hakkarainen K, and Parkkonen L, "On-scalp meg system utilizing an actively shielded array of optically-pumped magnetometers," *NeuroImage*, vol. 194, pp. 244–258, 2019. [PubMed: 30885786]

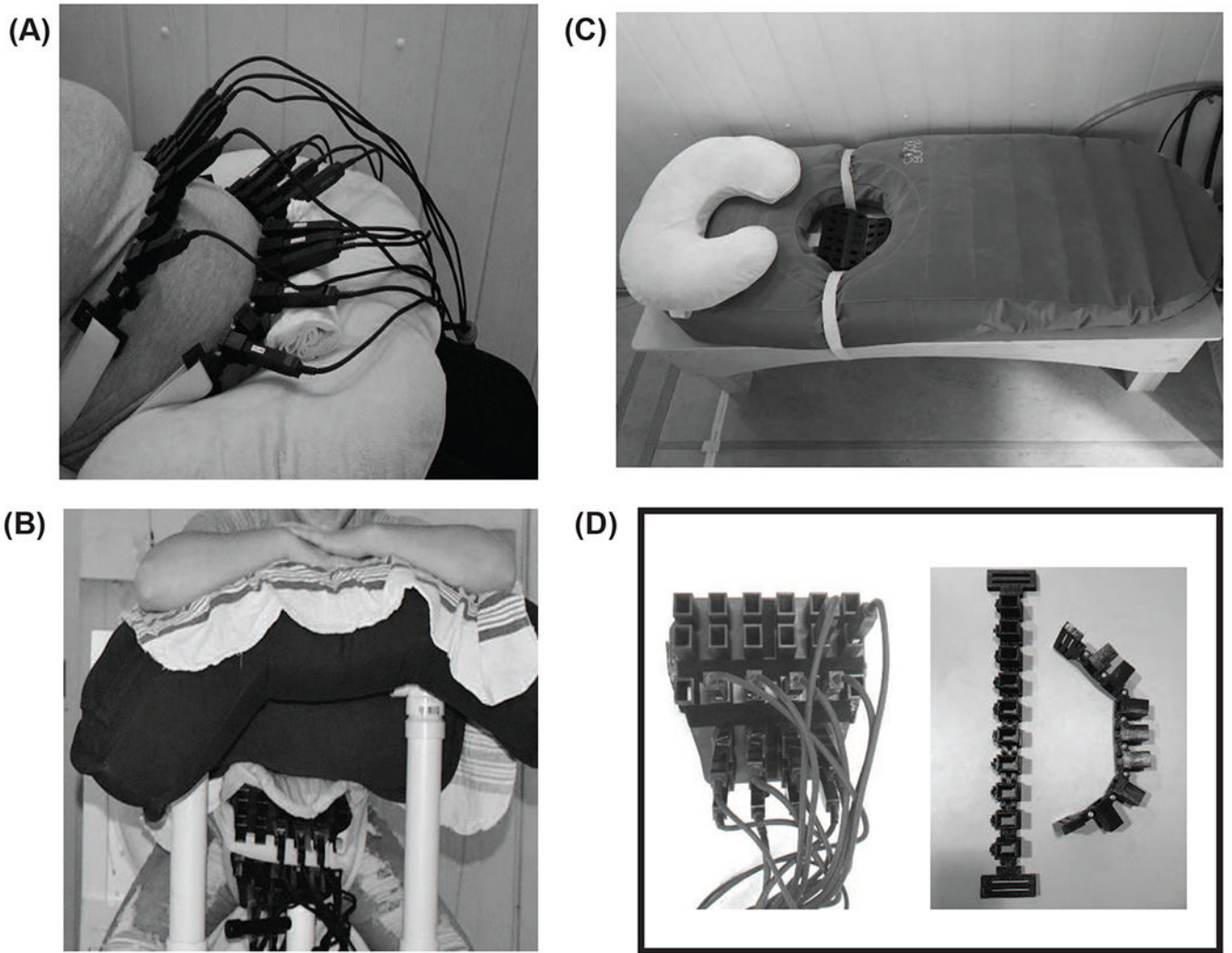


Fig. 1.
Pregnant woman positioned on OPM system. (A) (B)

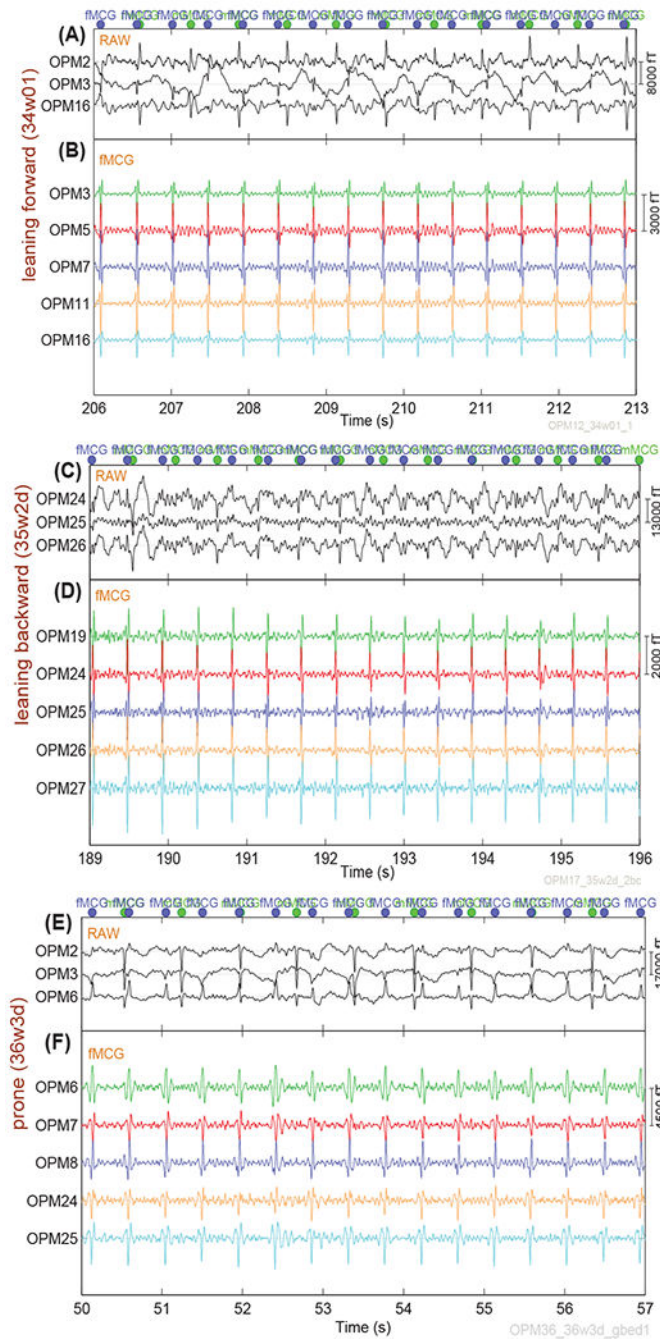


Fig. 2. 7s-fMCG signals from three datasets measured in the three positions at 34 (forward), 35 (backward) and 36 (prone) weeks GA. Raw time series are shown in (A, C, E) and the corresponding extracted fMCG signals in (B, D, F). Dots on the top of figures (A, C and E) represent the maternal (green dots) and fetal (blue dots) R peaks positions.

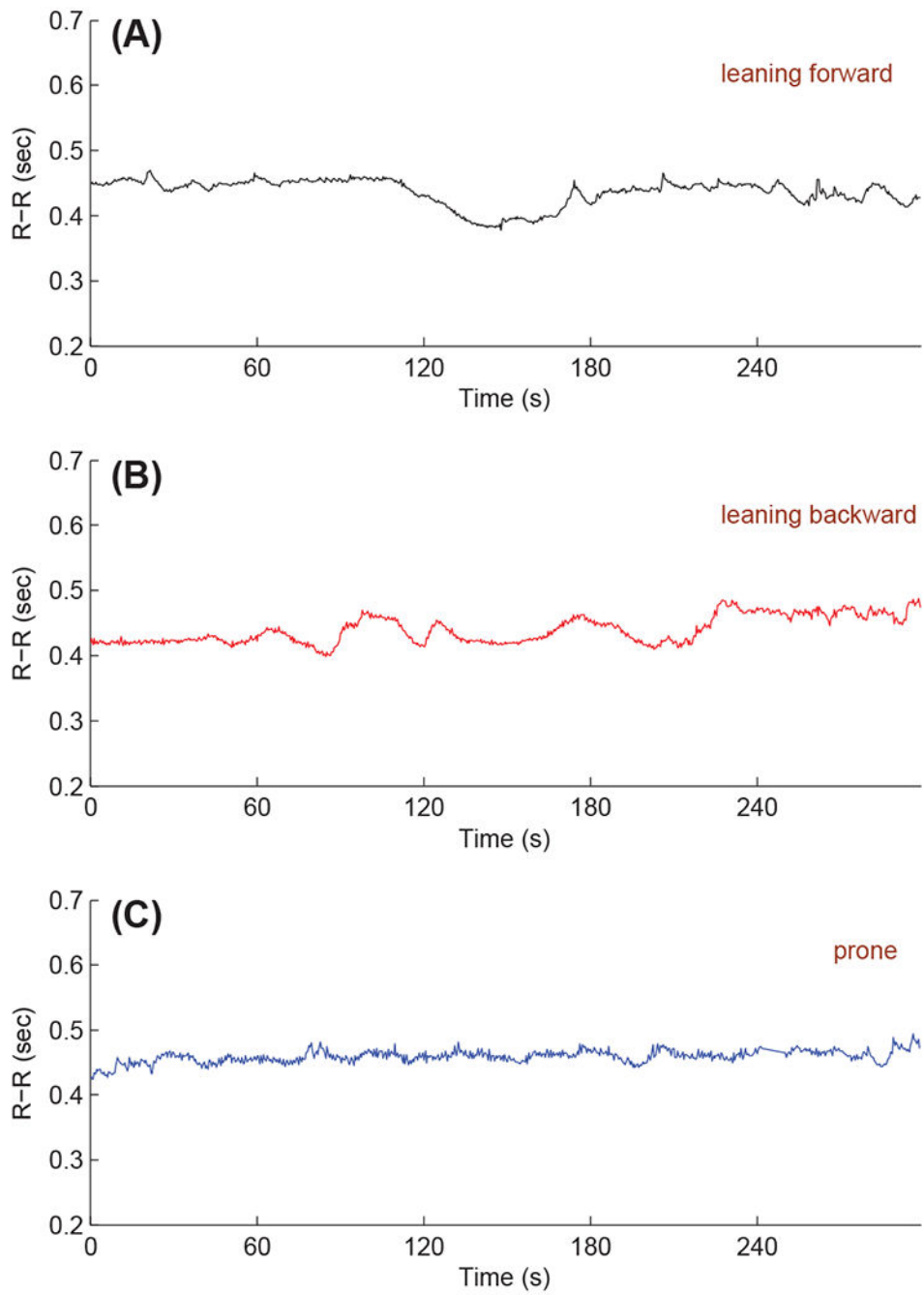


Fig. 3. R-R intervals measured in the three positions at 34 (backward), 35 (forward) and 36 (prone) weeks GA

TABLE I

FHRV ANALYSIS IN THE THREE POSITIONS AT 34 (BACKWARD), 35 (FORWARD) AND 36 (PRONE) WEEKS GA

Metric	forward	backward	prone
FHR (bpm)	138.2	137.1	130.8
R-R (ms)	435.2	438.5	458.8
RMSSD (ms)	3.5	4.7	7.1
SDNN (ms)	20.9	20.8	9.8

Author Manuscript

Author Manuscript

Author Manuscript

Author Manuscript